

Rheological Properties of a New Rubbery Nanocomposite: Polyepichlorohydrin/Organoclay Nanocomposites

Sang K. Lim, Ji W. Kim, I-J. Chin, Hyoung J. Choi

Department of Polymer Science and Engineering, Inha University, Incheon 402-751, Korea

Received 15 November 2001; accepted 10 May 2002

ABSTRACT: Nanocomposites of organophilic montmorillonite clay (OMMT) and polyepichlorohydrin (PECH) were intercalated by a solvent-casting method using dichloromethane as a solvent. The intercalation of PECH segments in the interlayers of the clay was confirmed by X-ray diffraction, and the intercalation spacing was calculated. The increase in the onset temperature of the thermal degradation indicated the enhancement of thermal stability of PECH due to intercalation. Rheological properties of the PECH/OMMT nanocomposites were investigated using a rotational rheometer in a steady shear mode. The steady shear viscosity

increased with the clay loading, and the shear thinning viscosity data were fitted well with the Carreau model. From the normalized shear viscosity analysis, a critical shear rate that is a crossover from a Newtonian plateau to a shear thinning region was found to approximately equal the inverse of the characteristic time of the nanocomposites. © 2002 Wiley Periodicals, Inc. *J Appl Polym Sci* 86: 3735–3739, 2002

Key words: intercalation; montmorillonite; polyepichlorohydrin; rheology; clay; nanocomposites

INTRODUCTION

Polymer nanocomposites are a new class of composites that are particle-filled polymers for which at least one dimension of the dispersed particles is in the nanometer range.^{1–5} In particular, polymer-layered silicate (PLS) nanocomposites belong to this category. Compared with the conventional microcomposites, PLS nanocomposites possess superior properties because of the maximized interfacial adhesion arising from the size characteristics of the silicate particles. These nanocomposites exhibit improved moduli, decreased thermal expansion coefficient, decreased gas permeability, increased swelling resistance, and enhanced ionic conductivity when compared with the pristine polymers,^{6–10} presumably because of the nanoscale structure of the nanocomposite and the synergism between the polymer and the silicate particles. The layered silicates commonly used in polymer nanocomposites belong to the structural family known as the 2 : 1 montmorillonite (MMT),¹¹ and the MMT has a high swelling capacity that is essential to achieve an efficient intercalation of the polymer¹² in the layered silicate. Because the interlayer of the pristine MMT is covered with sodium cation, the hydrophilicity is enhanced and could lead to high degree of swelling in water if an aqueous system is used during the intercalation procedure. Therefore, the emulsion

system containing an aqueous medium can maximize the affinity between the hydrophilic host in the clay and the hydrophobic guest of the monomer by the action of the emulsifier. Various polymer/clay nanocomposites created by emulsion polymerization have been reported; for examples, polyaniline,^{13,14} poly(methyl methacrylate),¹⁵ and styrene/acrylonitrile copolymer.^{16,17}

On the other hand, to render these hydrophilic MMT more organophilic, the hydrated cations of the interlayer can be exchanged with cationic surfactants,^{18,19} such as alkylammonium or alkylphosphonium ions (onium). As the modified clay (or organoclay) becomes organophilic, its surface energy is lowered and it becomes more compatible with organic polymers. These polymers can then be intercalated within the galleries, and this characteristic provides a way to prepare the rubber/clay nanocomposites in this study.

In general, rubber is a high molecular weight polymer with a very high viscosity in the processing state. Several rubbery polymer/clay nanocomposites have been investigated. Kojima et al.²⁰ prepared the butadiene–acrylonitrile copolymer/clay mixture by solvent-casting and then obtained the rubber/clay nanocomposite by mixing the clay intercalated with butadiene–acrylonitrile copolymer with the nitrile rubber under crosslinking conditions. Poly(styrene-*b*-butadiene) copolymer/clay nanocomposites have also been obtained with dioctadecyldimethyl ammonium MMT using a similar approach.²¹

Adopting a latex method, Wang et al.²² recently reported that clay could be dispersed in the rubber

Correspondence to: H.J. Choi (hjchoi@inha.ac.kr).

matrix, such as styrene–butadiene latex and styrene–vinylpyridine–butadiene latex, and that the clay could be used as a promising reinforcing agent in the rubber industry if it was dispersed on a nanometer scale. Furthermore, Yano and co-workers²³ found that the total path of the gas stream in the polyimide/organoclay nanocomposite film became much longer than that in the polyimide film using a conceptual equation proposed earlier. If the same equation is applied to our PECH/organoclay nanocomposite system, the total path of the gas stream in the nanocomposite film becomes 6.45 times that in the pristine polyepichlorohydrin (PECH).

In this study we prepared a new series of nanocomposites based on PECH and an organophilic clay (Cloisite25A) using a solvent-cast method, and then examined their thermal and rheological characteristics.

EXPERIMENTAL

Materials

PLS nanocomposites with organophilic clay and rubbery PECH were prepared by a solvent-cast method. PECH was purchased from Scientific Polymer Products (Ontario, NY) with an weight-average molecular weight (M_w) of 700,000 and a density of 1.36 g/cm³. The uncrystallizable, rubbery PECH, which is a homopolymer of epichlorohydrin, is a useful rubber that has an excellent resistance to ozone, oils, heat, and weathering, and also has a very low gas permeability. Recently, PECH has been reported to be miscible with biodegradable polymers such as polyhydroxybutyrate²⁴ and synthetic aliphatic polyester.^{25,26} Dichloromethane from Sam-Chun Chemical (Korea) was used without any purification. The commercially available organophilic clay (Cloisite 25A) produced by Southern Clay Products (Gonzales, TX) was used as the layered silicate in which the pristine Na⁺-MMT was treated by a cation-exchange reaction with dimethyl hydrogenated-tallow (2-ethylhexyl) quaternary ammonium methylsulfate. Organoclay was dried under vacuum at 100°C prior to use to remove the residual water completely. Wide-angle X-ray scattering (WAXS) using a rotating anode source was used to investigate the insertion of PECH between the clay layers, and differential scanning calorimetry (DSC) was used to measure the glass-transition temperature.

Nanocomposite preparation

The polymer/clay nanocomposites are known to be greatly dependent on the dispersion behavior of the MMT particles. Thus, organoclay was dispersed in 200 mL of dichloromethane and sonicated for 60 min with an ultrasonic generator (Kyung-III ultrasonic Com-

pany, Korea) consisting of magnetostrictive probe-type transducers (vibrator) operated at a nominal frequency of 28 kHz and equipped with a temperature controller. The mixture of 0.4 g of organoclay and 200 mL of dichloromethane was stirred for 48 h at room temperature. Simultaneously, 19.6 g of PECH was added to 300 mL of dichloromethane and stirred for 48 h at room temperature. The two solutions were then mixed together. After stirring vigorously for 48 h at room temperature, the solution mixture was poured into a glass Petri dish. Three samples of nanocomposites, marked PECL 2, PECL 5, and PECL 10, were prepared employing 2, 5, and 10% by weight, respectively of the organophilic clay with respect to the total nanocomposite weight.

Characterization

X-ray diffraction (XRD), which is widely employed for the characterization of nanocomposites, verified the insertion of PECH between the layers of clay. A Guinier focusing camera, with a quartz crystal monochromator in a Philips PW1847 X-ray crystallographic unit and fitted with a copper target, was used (40 kV, 20 mA) to record X-ray patterns in the range $2\theta = 1.5\text{--}10^\circ$ with a scan rate of $2^\circ/\text{min}$. Amount of polymer loading was measured by thermogravimetric analysis (TGA) using a Polymer Laboratories TGA1000.

Rheological behavior in a steady shear flow field is known to be related to the extent of the distortion/deformation of nanocomposites. Despite its importance, the rheological behavior of polymer/clay nanocomposites as a function of the intercalated/exfoliated structure has not been well studied.^{27,28} For a steady shear strain experiment, we used a Physica MC120 (Germany) rotational rheometer with a parallel plate geometry (25-mm diameter plates) at 200°C. Steady shear viscosity was obtained as a function of the shear rate in the CSR (controlled shear rate) mode.²⁹

RESULTS AND DISCUSSION

The variation of the (001) *d*-spacing of the clay interlayer of the nanocomposites, which was calculated from the observed peaks by using the Bragg formula,³⁰ is shown in Figure 1. The interlayer spacing increased from 18.4 Å for the base distance of the clay itself to 59.3, 69.4, and 68.9 Å for PECL2, PECL5, and PECL10 nanocomposites, respectively, due to the insertion of the PECH. The *d*-spacing of 18.4 Å for the OMMT is greater than that of the pristine Na⁺-MMT (9.7 Å),⁸ which would ease the intercalation of monomer or polymer molecules in the clay layers. The increased *d*-spacing would also lead to easy dissociation of MMT, resulting in hybrids with better dispersion of clay particles.

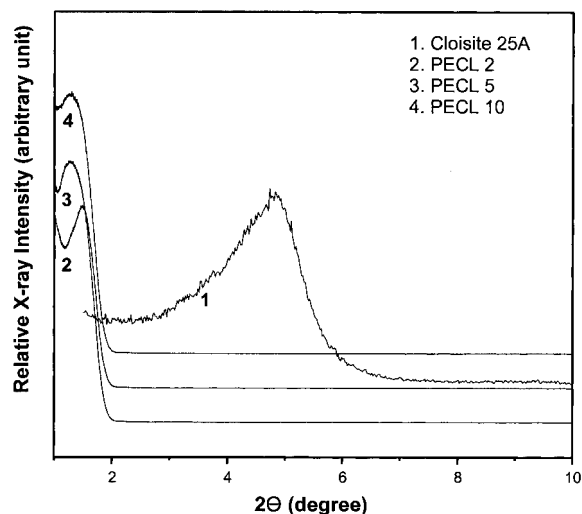


Figure 1 X-ray diffraction patterns of organoclay and nanocomposites.

The TGA thermograms for PECH and nanocomposites are shown in Figure 2. The onset of thermal decomposition of nanocomposites shifted significantly toward higher temperatures compared with that of PECH, which confirms the enhancement of thermal stability of the intercalated PECH. The decomposition onset temperatures of the PECH/OMMT nanocomposites for PECL 2 and PECL 5 were 326 and 328°C, respectively, and they are higher than that of PECH (268°C). The shift of the onset temperature of the thermal degradation might indicate a decrease in permeability for oxygen or volatile degradation products, which could be due to the action of the homogeneously incorporated and distributed clay sheets.³¹ Indeed, the nanoscale MMT layers may prevent the

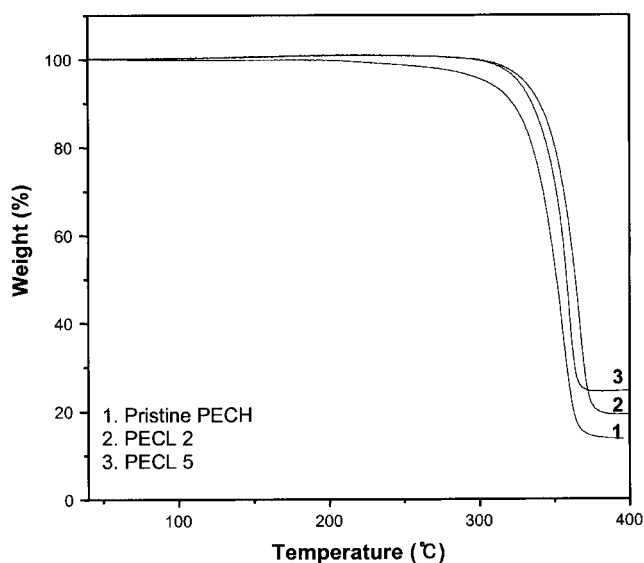


Figure 2 TGA thermograms for pure PECH and nanocomposites.

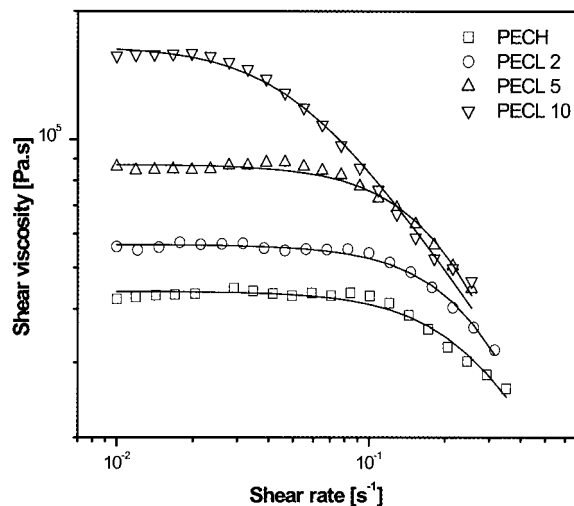


Figure 3 Steady shear viscosity of pure PECH as a function of shear rate. (Lines represent the curve-fitting results based on eq. 1.)

diffusion of volatile decomposition products, and the pathways of volatile decomposition products can increase significantly in the PECH/OMMT nanocomposites.³¹ These phenomena may be the reason why the PECH/OMMT nanocomposites exhibit higher thermal stability than pure PECH. The thermal behavior of the PECH/OMMT nanocomposites are consistent with the earlier report³² that the intercalated polymers affect the thermal properties of the layered host.

The steady shear viscosities measured in the molten state at 200°C for pure PECH and PECH/clay nanocomposites with different amounts of OMMT clay loading are shown in Figure 3. The shear viscosities of PECH/clay nanocomposites are higher than that of pure PECH, regardless of the OMMT loading. This enhancement arises because of the interaction and dispersion of organophilic clay in the polymer matrix, which appears to provide resistance to flow and deformation of the molten polymer. According to these results, clay particles in the PECH/clay nanocomposite are considered to be homogeneously dispersed. The shear viscosity increased substantially with the clay content at low shear rates. On the other hand, at high shear rates, the nanocomposites display a rapid shear-thinning behavior that is comparable to that of the pure polymer because the entanglement of polymer chain and the arrangement of clay particles are not permanent and they can be altered under flow and during relaxation processes.^{33,34} Similar steady shear rheological behavior has been also investigated for a series of intercalated poly(dimethyl-diphenyl siloxane)-layered silicate (dimethyl-ditallow MMT) nanocomposites with varying silicate loadings.³⁵

To investigate the dependence of the shear viscosity (η) on the shear rate ($\dot{\gamma}$), we fitted the measured shear viscosity to the Carreau model³⁶ given in the following equation:

$$\eta = \frac{\eta_0}{[1 + (\dot{\gamma}\lambda)^2]^{(1-n)/2}} \quad (1)$$

where η_0 is the zero shear rate viscosity, λ is the characteristic time, and n is a dimensionless parameter. The slope in the power-law region is given by $n - 1$. Note that in the special case of $n = 1$ or $\dot{\gamma}\lambda \rightarrow 0$, this model reduces to the Newtonian fluid model possessing constant viscosity, and if $n < 1$, the model predicts a shear-thinning behavior.³⁷ The values of η_0 and λ that were obtained from the curve fitting of the experimental data in Figure 3 to eq. 1 are listed in Table I. In Figure 3, the shear-thinning behavior and the zero shear rate viscosity drastically increased with the clay loading of 10 wt %. A transition from the low shear plateau to the power-law behavior was also evident, which may be due to alignment and orientation of clay particles.³⁸ The shear thinning viscosities of biodegradable aliphatic polyester/poly(vinyl acetate) blends,³⁹ poly(3-hydroxybutyrate) and PEO blends,⁴⁰ and poly(ethylene oxide)-clay nanocomposites³³ have been reported to fit well with the Carreau model.

The normalized shear viscosities (shear viscosity divided by the corresponding zero-shear viscosity η_0 , which was obtained from the Carreau model) as a function of the shear rate, demonstrating a Newtonian plateau at low shear rates and a power-law behavior at high shear rates, are shown in Figure 4. For PECH/OMMT in the melt state, a crossover from a Newtonian plateau to a shear-thinning region occurs at a critical shear rate, $\dot{\gamma}_c$.⁴¹ Furthermore, $\dot{\gamma}_c$ is approximately equal to the inverse of the characteristic time of the PECH/OMMT nanocomposite, which is the longest relaxation time required for the elastic structures of the PECH/OMMT nanocomposite. The values of $\dot{\gamma}_c$ are 0.092, 0.121, 0.084, and 0.015 s⁻¹ for PECH, PECL 2, PECL 5, and PECL 10, respectively. We found that there is a strong correlation between λ and $\dot{\gamma}_c$ for PECH/OMMT. We could postulate that $\lambda\dot{\gamma}_c$ is a universal constant with a value of 0.3, where λ depends on both the clay volume fraction and its nanostructure. The constant value of $\lambda\dot{\gamma}_c \cong 0.3$ is illustrated in Figure 4. A similar concept has been introduced to describe an anomalous lateral migration of a rigid sphere in a torsional flow.⁴² Although the exact mechanism that causes shear-thinning is not fully under-

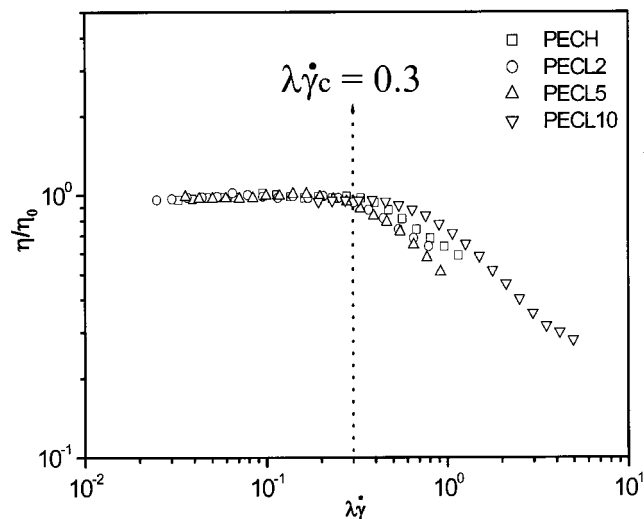


Figure 4 η/η_0 versus $\lambda\dot{\gamma}$; of pure PECH and nanocomposites.

stood, we conjecture that it might be due to the orientation of silicate layers and polymer coils under shear. With increasing the shear rates, the conformations of the intercalated chains are expected to change as the coils align parallel to the direction of the flow.^{43–45}

CONCLUSIONS

We prepared the rubbery PECH/organoclay nanocomposites and examined the change in the clay interlayer spacing as a function of the clay loading. The thermal stability of the PECH/organoclay nanocomposite increased with the clay content. From the rheological measurements, an increase in the shear viscosity of nanocomposites was observed with an increase in the organoclay loading. Furthermore, the PECH/organoclay nanocomposite exhibited more rapid shear thinning behavior than pure PECH, which might result from the reorientation of dispersed clay particles.

We acknowledge the financial support from Inha University through a special funding program of 2000. One of the authors (H. J. Choi) also appreciates research grants from the Korea Science and Engineering Foundation (KOSEF) through the Applied Rheology Center (ARC), an official KOSEF-created engineering research center (ERC) at Korea University, Korea.

References

- Gleiter, H. *Adv Mater* 1992, 4, 474.
- Djoković, V.; Nedeljković, J.M. *Macromol Rapid Commun* 2000, 21, 994.
- Hoffmann, B.; Kressler, J.; Stöppelmann, G.; Fridrich, Chr.; Kim, G.M. *Colloid Polym Sci* 2000, 278, 629.
- Ziolo, R.F.; Gianellis, E.P.; Weinstein, B.A.; O'Horo, M.P.; O'Horo, B.N.; Mehrotra, V.; Huffman, D.R. *Science* 1992, 219, 257.

TABLE I

Zero Shear Rate Viscosity and Characteristic Time for the PECH/OMMT Nanocomposites

Sample Code	η_0 (Pa · s) $\times 10^{-5}$	λ (s)
PECH	0.44	3.27
PECL 2	0.57	2.49
PECL 5	0.87	3.58
PECL 10	1.65	19.36

5. Chin, I.J.; Thurn-Albrecht, T.; Kim, H.C.; Russell, T.P.; Wang, J. *Polymer* 2001, 42, 5947.
6. Heinemann, J.; Reichert, P.; Thomann, R.; Mülhaupt, R. *Macromol Rapid Commun* 1999, 20, 423.
7. Ryu, J.G.; Lee, P.S.; Kim, H.; Lee, J.W. *Korea-Australia Rheol J* 2001, 13, 61.
8. Strawhecker, K.E.; Manias, E. *Chem Mater* 2000, 12, 2943.
9. Gilman, J.W.; Jackson, C.L.; Morgan, A.B.; Harris, R.; Manias, E.; Giannelis, E. P.; Wuthenow, M.; Hilton, D.; Phillips, S.H. *Chem Mater* 2000, 12, 1866.
10. Kim, B.H.; Jung, J.H.; Joo, J.; Epstein, A.J.; Mizoguchi, K.; Kim, J.W.; Choi, H.J. *Macromolecules* 2002, 35, 1419.
11. Grim, R.E. *Clay Mineralogy*; McGraw-Hill: New York, 1953; p. 137.
12. Kormann, X.; Berglund, L.A.; Sterte, J.; Giannelis, E.P. *Polym Eng Sci* 1998, 8, 38.
13. Kim, J.W.; Kim, S.G.; Choi, H.J.; Jhon, M.S. *Macromol Rapid Commun* 1999, 20, 450.
14. Kim, B.H.; Jung, J. H.; Kim, J. W.; Choi, H. J.; Joo, J. *Synth Met* 2001, 117, 115.
15. Lee, D.C.; Jang, L.W. *J Appl Polym Sci* 1996, 61, 1117.
16. Kim, J.W.; Noh, M.H.; Choi, H.J.; Lee, D.C.; Jhon, M.S. *Polymer* 2000, 41, 1229.
17. Kim, J.W.; Choi, H.J.; Jhon, M.S. *Macromol Symp* 2000, 155, 229.
18. Hoffmann, B.; Dietrich, C.; Thomann, R.; Friedrich, C.; Mülhaupt, R. *Macromol Rapid Commun* 2000, 21, 57.
19. Chen, G.; Liu, S.; Zhang, S.; Qi, Z. *Macromol Rapid Commun* 2000, 21, 746.
20. Kojima, Y.; Fukumori, K.; Usuki, A.; Okada, A.; Kurauchi, T. *J Mater Sci Lett* 1993, 12, 889.
21. Laus, M.; Francescangeli, O.; Sandrolini, F. *J. Mater Res* 1997, 12, 3134.
22. Wang, Y.; Zhang, L.; Tang, C.; Yu, D. *J Appl Polym Sci* 2000, 78, 1879.
23. Yano, K.; Usuki, A.; Okada, A. *J. Polym Sci, Part A: Polym Chem* 1997, 35, 2289.
24. Verhoogt, H.; Ramsay, B.A.; Favis, B.D. *Polymer* 1994, 35, 5155.
25. Kim, J.; Shin, T.G.; Choi, H.J.; Jhon, M.S. *Polymer* 1999, 40, 6873.
26. Kim, J.; Lim, S.T.; Choi, H.J.; Jhon, M.S. *Macromol Chem Phys* 2001, 202, 2634.
27. Giannelis, E.P.; Krishnamoorti, R.; Manias, E. *Adv Polym Sci* 1999, 138, 107.
28. Solomon, M.J.; Almusallam, A.S.; Seefeldt, K.F.; Somwangth-anaroj, A.; Varadan, P. *Macromolecules* 2001, 34, 1864.
29. Choi, H.J.; Cho, M.S.; Kim, J.W. *Korea-Australia Rheol J* 2001, 13, 197.
30. Zanetti, M.; Lomakin, S.; Camio, G. *Macromol Mater Eng* 2000, 279, 1.
31. Chen, G.; Liu, S.; Qi, Z. *Macromol Chem Phys* 2001, 202, 1189.
32. Komori, Y.; Sugahara, Y.; Kuroda, K. *J Mater Chem* 1999, 9, 3081.
33. Choi, H.J.; Kim, S.G.; Hyun, Y.H.; Jhon, M.S. *Macromol Rapid Commun* 2001, 22, 320.
34. Lim, S.T.; Hyun, Y.H.; Choi, H.J.; Jhon, M.S. *Chem Mater* 2002, 14, 1839.
35. Krishnamoorti, R.; Vaia, R.A.; Giannelis, E.P. *Chem Mater* 1996, 8, 1728.
36. Carreau, P.J.; De Kee, D.C.; Chhabra, R.P. *Rheology of Polymeric Systems Principle and Applications*; Hanser Publisher: New York, 1997.
37. Lau, A. K. M.; Tiu, C.; Kealy, T.; Tan, K.C. *Korean-Australia Rheol J* 2002, 14, 1.
38. Chen, G.; Qi, Z. *J Mater Res* 2000, 15, 351.
39. Shin, T.K.; Kim, J.; Choi, H.J.; Jhon, M.S. *J Appl Polym Sci* 2000, 77, 1348.
40. Park, S.H.; Lim, S.T.; Shin, T.K.; Choi, H.J.; Jhon, M.S. *Polymer* 2001, 42, 5737.
41. Hyun, Y.H.; Lim, S.T.; Choi, H.J.; Jhon, M.S. *Macromolecules* 2001, 34, 8084.
42. Choi, H.J.; Prieve, D.C.; Jhon, M.S. *J Rheol* 1987, 31, 317.
43. Manias, E.; Hadziioannou, G.; Brinke, G. *Langmuir* 1996, 12, 4587.
44. Krishnamoorti, R.; Ren, J.; Silva, A. S. *J Chem Phys* 2001, 114, 4968.
45. Kim, T.H.; Jang, L.W.; Lee, D.C.; Choi, H.J.; Jhon, M.S. *Macromol Rapid Commun* 2002, 23, 191.